Article:

Xiao, Q. orcid.org/0000-0002-7386-3793, Tan, Z. and Du, M. (2024) Probabilistic optimal power flow computation for power grid including correlated wind sources. IET Generation, Transmission & Distribution, 18 (14). pp. 2383-2396. ISSN 1751-8687

https://doi.org/10.1049/gtd2.13196

Received: 18 March 2024 | Revised: 13 May 2024 | Accepted: 20 May 2024

IET Generation, Transmission & Distribution

DOI: 10.1049/gtd2.13196

The Institution of Engineering and Technology WILEY

ORIGINAL RESEARCH

Probabilistic optimal power flow computation for power grid including correlated wind sources

Qing Xiao[1] | Zhuangxi Tan[1] | Min Du[2]

[1]School of Information and Electrical Engineering, Hunan University of Science and Technology, Xiangtan, Hunan Province, China

[2]Department of Automatic Control and Systems Engineering, University of Sheffield, Sheffield, South Yorkshire, UK

Correspondence
Qing Xiao, School of Information and Electrical Engineering, Hunan University of Science and Technology, Xiangtan, Hunan Province, China.
Email: qxiao@mail.hnust.edu.cn

Min Du, Department of Automatic Control and Systems Engineering, University of Sheffield, Sheffield, South Yorkshire, UK.
Email: m.du@sheffield.ac.uk

Funding information
National Natural Science Foundation of China, Grant/Award Number: 12271155; Doctoral Research Start-up Fund of Hunan University of Science and Technology, Grant/Award Number: E52170

Abstract
This paper sets out to develop an efficient probabilistic optimal power flow (POPF) algorithm to assess the influence of wind power on power grid. Given a set of wind data at multiple sites, their marginal distributions are fitted by a newly developed generalized Johnson system, whose parameters are specified by a percentile matching method. The correlation of wind speeds is characterized by a flexible Liouville copula, which allows to model the asymmetric dependence structure. In order to improve the efficiency for solving POPF problem, a lattice sampling method is developed to generate wind samples at multiple sites, and a logistic mixture model is proposed to fit distributions of POPF outputs. Finally, case studies are performed, the generalized Johnson system is compared with Weibull distribution and the original Johnson system for fitting wind samples, Liouville copula is compared against Archimedean copula for modelling correlated wind samples, and lattice sampling method is compared with Sobol sequence and Latin hypercube sampling for solving POPF problem on IEEE 118-bus system, the results indicate the higher accuracy of the proposed methods for recovering the joint cumulative distribution function of correlated wind samples, as well as the higher efficiency for calculating statistical information of POPF outputs.

1 | INTRODUCTION

The continuous variation of wind speed leads to the fluctuation of the output of wind farms [1, 2]. When wind turbines are connected to the electric grid, the probabilistic optimal power (POPF) model can serve as a candidate tool to handle the uncertain behaviour of wind power, which deploys statistical methods to describe the variation of wind speeds [3]. In practical settings, wind speeds at neighbouring sites are correlated and non-normally distributed, the implementation of POPF computation would bring forward the issue of modelling correlated wind speeds, where the use of copula is often suggested [4, 5].

In the framework of copula theory, the joint cumulative distribution function (CDF) of wind speeds can be recovered by marginal distributions and its dependence structure. Hence, given a set of wind speed data, the first step would be to fit marginal CDFs of wind samples. The employed statistical model should meet the following requirements:

1) it can accurately match the statistical information of wind samples at each site;
2) its parameters can be conveniently determined;
3) its CDF, probability density function (PDF) and quantile function (QF) can be given in closed form, which helps to generate samples for POPF computation.

Hitherto, several statistical models have been suggested for fitting wind speed samples, such as: Weibull distribution [6, 7], Burr distribution [8], Kappa distribution [9], generalized lambda distribution (GLD) [10], Johnson system [11], Cornish–Fisher expansion [12], polynomial transformation model (PTM) [13, 14], Gram–Charlier series [15], kernel tuned polynomial expansion (KTPE) series [16], kernel density estimate method [17, 18],

TABLE 1 A summary of statistical models for fitting wind speed samples.

		Distribution functions			Parameter estimation algorithms			
Type	**Model**	**CDF**	**PDF**	**QF**	**MLE**	**RM**	**PWM**	**Percentile**
I	Weibull distribution	√	√	√	√	√	√	√
	Burr distribution	√	√	√	√	×	×	×
	Kappa distribution	√	√	√	×	×	×	√
	GLD	×	×	√	√	√	√	√
	Johnson system	√	√	√	×	√	×	√
	Cornish–Fisher expansion	×	×	√	×	√	×	×
	PTM	×	×	√	×	×	√	√
II	Gram–Charlier series	√	√	×	×	√	×	×
	KTPE	√	√	×	×	×	×	√
	KDE	√	√	×	√	×	×	×
	GMM	√	√	×	√	×	×	√

and Gaussian mixture model (GMM) [19, 20]. These models are summarized in Table 1, which are classified into two types: type-I and type-II.

Let X denote the wind speed, type-I models aim to relate X to another random variable with a known CDF, which makes it easy to generate wind speed samples. Taking Weibull distribution for example, its quantile function (QF) is in closed form, the wind speed X can be explicitly related to a standard uniform variable, and wind speed samples can be generated by applying QF to standard uniform deviates. From this viewpoint, the underlying idea of Johnson system and Cornish–Fisher is the same, because both of them characterize the uncertainty of wind speed by relating X to a standard normal variable. When fitting wind speed data, type-I models can be parameterized by the maximum likelihood estimation (MLE) method, raw moment (RM) matching, probability weighted moment (PWM) matching or percentile matching method, which are summarized in Table 1.

The type-II models set out to reconstruct the CDF and PDF of wind speed in closed form, but the quantile function cannot be analytically given, when it comes to generating wind speed samples, numerical algorithms should be introduced to calculate the quantile function. Besides, except for Gram–Charlier series, the parameters of type-II model are difficult to be determined by the moment matching method, algorithms like MLE method and percentile matching method should be deployed to tackle this problem.

Once marginal distributions are fitted, the joint CDF of wind speeds can be constructed by elliptical copula or Archimedean copula. The elliptical copula is developed from an multivariate elliptical distribution, which is capable of characterizing the mutual dependence structure of wind speeds. One advantage of elliptical copula is that analytical formula is readily available to parameterize the copula model and to generate correlated samples. Although a theoretical framework has been proposed to construct different elliptical copulas, only a few of them have a joint PDF in closed form, which includes Gaussian copula [21], t-copula [22] and Laplace copula [14].

In contrast to elliptical copula, most Archimedean copulas have a joint CDF in closed form, and Archimedean copulas derived from different generators can be used to represent different types of dependence structures of wind speeds. If Kendall's τ is employed to measure the dependence structure of wind samples, the parameters of Archimedean copula can be obtained analytically [4, 23]. The main problem of Archimedean copula is that it lacks a generic and efficient sample generation algorithm. Generic algorithms like Rosenblatt transformation and rejection sampling method can be used to sample Archimedean copulas based on various generators, but they are not computationally convenient [16]; the algorithm based on Laplace transformation is very efficient, but it is mathematically demanding, and only applicable to a few Archimedean copulas [9]. Therefore, when Archimedean copula is employed to model correlated wind speeds, more efforts should be devoted to developing efficient and convenient algorithms to sample Archimedean copula.

Once the stochastic behaviour of wind speeds is represented by copula, POPF computation can be implemented to measure the influence of wind speed variation on electric grid. The POPF regards uncertain variables in the optimal power flow (OPF) model as inputs, and calculates statistical information of OPF solutions to quantify the uncertainty effects of inputs [6, 7]. Mathematically, the POPF model is a black-box system with random inputs, solutions of OPF model can be regarded as POPF outputs. Hitherto, various uncertainty quantification algorithms have been introduced to estimate statistical moments or distribution functions of POPF outputs, which can also be classified into two types.

The underlying idea of type-I algorithms is to deploy statistical moments to represent the stochastic behaviour of POPF inputs, such as: cumulant method [24], point estimate method (PEM) [25, 26] and unscented transformation (UT) method [27]. When the cumulant method is used for POPF computation, it establishes a linear model to calculate cumulants of POPF outputs from those of inputs. This strategy is extremely efficient, and requires only one deterministic OPF computation, but it does not work very well when the stochastic variation of POPF inputs is large. In order to improve the accuracy, PEM and UT employ a non-linear polynomial model to relate POPF inputs and outputs [28]. However, the number of POPF inputs is generally large, and the curse of dimensionality would arise during POPF computation, therefore, the emphasis of type-I algorithms is to balance the accuracy and computational burden.

The type-II algorithms include Monte Carlo simulation (MCS) [17], quasi-Monte Carlo simulation (QMCS) [22] and Latin hypercube sampling (LHS) [16]. The basic idea of these algorithms is to generate samples to represent statistical features of wind speeds. Via copula method and marginal transformations, the POPF problem with m inputs can be mapped to an m-dimensional hypercube space, where the difference of these three algorithms can be illustrated. MCS generates samples of POPF inputs from a pseudorandom sequence, which may cluster in some regions and leave gaps in other regions, leading to a low convergence rate in the case of POPF computation. In comparison with MCS, QMCS and LHS employ low discrepancy sequences to generate samples of POPF inputs, which are more uniformly distributed in the m-dimensional hypercube space $[0,\ 1]^m$. When QMCS and LHS are used to solve POPF problem, their computation burden is lower than that of MCS.

This paper aims to develop an efficient POPF computation algorithm to assess the influence of wind power on power grid, and wind speeds are regarded as POPF inputs. The contributions are summarized as follows:

1) In the case that only samples of POPF inputs are available, a generalized Johnson system is proposed to recover distribution functions of POPF inputs.
2) A new copula model named Liouville copula is employed to decouple correlated POPF inputs to independent standard uniform random variables, which allows for characterizing the asymmetric and symmetric dependence structure of POPF inputs.
3) A lattice sampling method is developed to generate low discrepancy sequences, and to efficiently solve the POPF problem.

The following part of the paper is organised as follows. Section 2 derives the generalized Johnson system. Section 3 develops a Liouville copula based on Clayton generator to model correlated wind speeds. Section 4 presents lattice sampling method and logistic mixture model (LMM) to solve the POPF problem. Section 5 performs case study to verify the proposed methods, and the related conclusions are given in Section 6.

2 | GENERALIZED JOHNSON SYSTEM

This section aims to develop a class of statistical models to recover the CDF, PDF and quantile function of wind samples. Consider the original Johnson system based on the standard normal distribution

$$X = J(Z) = \begin{cases} a + b \cdot sinh\left(\dfrac{Z-c}{d}\right) & S_U \\ a + b \cdot exp\left(\dfrac{Z-c}{d}\right) & S_L \\ a + b - \dfrac{b}{1 + exp\left(\frac{Z-c}{d}\right)} & S_B, \end{cases} \tag{1}$$

where X represents the target wind speed, Z denotes a standard normal variable, a, b, c and d are parameters.

The Johnson system in Equation (1) can be viewed like this: it first deploys the normal distribution to fit wind samples, and then improves the fitting by using an appropriate model in Equation (1). Because wind speed generally follows a non-normal distribution, if the normal distribution in Equation (1) is replaced by a more appropriate distribution, say, Weibull distribution, it can yield a better representation for the wind speed. This paper proposes a generalized Johnson system by assuming Z to be a non-normal random variable with zero mean.

Let $\Psi(Z)$ be the CDF of Z, let $F(X)$ be the CDF of wind speed. If the analytical expression of $\Psi(Z)$ is known, it has

$$F(X) = \Psi(Z) = \Psi\left[J^{-1}(X)\right], \tag{2}$$

where $J^{-1}(\cdot)$ is the inverse of $J(\cdot)$ in Equation (1)

$$Z = J^{-1}(X) = \begin{cases} c + d \cdot sinh^{-1}\left(\dfrac{X-a}{b}\right) & S_U \\ c + d \cdot ln\left(\dfrac{X-a}{b}\right) & S_L \\ c + d \cdot ln\left(\dfrac{X-a}{a+b-X}\right) & S_B. \end{cases} \tag{3}$$

Then, the PDF of wind speed is

$$\begin{aligned} f(X) &= \frac{d[F(X)]}{dX} = \frac{d[\Psi(Z)]}{dZ} \cdot \frac{dZ}{dX}\bigg|_{Z=J^{-1}(X)} \\ &= \begin{cases} \psi\left[J^{-1}(X)\right] \cdot \dfrac{d}{\sqrt{(X-a)^2+b^2}} & S_U \\ \psi\left[J^{-1}(X)\right] \cdot \dfrac{d}{X-a} & S_L \\ \psi\left[J^{-1}(X)\right] \cdot \dfrac{bd}{(X-a)(a+b-X)} & S_B, \end{cases} \end{aligned} \tag{4}$$

where $\psi(\cdot)$ is the PDF of Z. The quantile function of wind speed is

$$X = F^{-1}(U) = J\left[\Psi^{-1}(U)\right], \tag{5}$$

where U is a uniform variable within the range $[0,\ 1]$, $F^{-1}(\cdot)$ and $\Psi^{-1}(\cdot)$ are quantile functions of X and Z, respectively.

If Z in Equation (1) is a non-normal random variable, the algorithm in reference [29] cannot be used to parameterize the proposed model. In Appendix, a generalized Johnson system based on Weibull distribution is presented in Table A1, and a percentile matching method is presented for the parameter estimation.

3 | LIOUVILLE COPULA

3.1 | Model construction

Consider correlated wind speeds at d different sites, let $F_i(X_i)$ be the CDF of X_i $(i = 1, \dots, d)$, then a correlated standard uniform random vector $\boldsymbol{U}$ can be obtained by

$$\boldsymbol{U} = \begin{pmatrix} U_1 \\ \vdots \\ U_i \\ \vdots \\ U_d \end{pmatrix} \xleftarrow{U_i = F_i(X_i)} \begin{pmatrix} X_1 \\ \vdots \\ X_i \\ \vdots \\ X_d \end{pmatrix}, \tag{6}$$

where U_i is a uniform variable within [0, 1] $(i = 1, \dots, d)$. Let $\boldsymbol{C}_d(\boldsymbol{U})$ denote the employed copula model, let $\boldsymbol{F}_d(\boldsymbol{X})$ be the joint CDF of wind speeds, it has

$$\begin{aligned} \boldsymbol{F}_d(\boldsymbol{X}) &= \boldsymbol{C}_d(U_1, \dots, U_i, \dots, U_d) \\ &= \boldsymbol{C}_d\left[F_1(X_1), \dots, F_i(X_i), \dots, F_d(X_d)\right]. \end{aligned} \tag{7}$$

If the elliptical copula or Archimedean copula is used to construct $\boldsymbol{C}_d(\cdot)$ and to generate samples of correlated wind speeds for POPF computation, it has

$$\begin{pmatrix} V_1 \\ \vdots \\ V_i \\ \vdots \\ V_d \end{pmatrix} \xrightarrow{\text{Copula}} \begin{pmatrix} U_1 \\ \vdots \\ U_i \\ \vdots \\ U_d \end{pmatrix} \xrightarrow{X_i = F_i^{-1}(U_i)} \begin{pmatrix} X_1 \\ \vdots \\ X_i \\ \vdots \\ X_d \end{pmatrix}, \tag{8}$$

where $\boldsymbol{V} = (V_1, \dots, V_i, \dots, V_d)$ is a d-dimensional independent uniform random vector, and the quantile function $F_i^{-1}(\cdot)$ can be constructed by the generalized Johnson system in Equation (5) $(i = 1, \dots, d)$. With Equation (8), samples of $\boldsymbol{V}$ can be transformed to samples of correlated wind speeds, and the POPF problem can be mapped to the independent uniform space.

Instead of elliptical copula and Archimedean copula, this paper employs Liouville copula to construct the joint CDF of wind speeds, and sets out to relate $\boldsymbol{U}$ to a D-dimensional random vector $\boldsymbol{V} = (V_1, \dots, V_i, \dots, V_D)$ $(D \geq d)$. In other words, Liouville copula employs D $(D > d)$ independent uniform variables to fit the dependence structure of $\boldsymbol{X}$, which is expected to enhance the flexibility of the copula and allows for a better representation of correlated wind speeds.

3.2 | Sample generation

Here, a Liouville copula based on Clayton generator is constructed to represent the dependence structure of wind speeds. The following presents the analytical expression of Clayton generator

$$\phi(t) = (1 + t)^{-\frac{1}{\theta}}, \tag{9}$$

where θ is the parameter.

Let $\boldsymbol{X} = (X_1, \dots, X_i, \dots, X_d)$ denote correlated wind speeds, suppose wind speed at the ith site is represented by α_i different independent uniform variables, the dependence structure of $\boldsymbol{X}$ would be characterized by Clayton generator and a D-dimensional independent standard uniform random vector $\boldsymbol{V} = (V_1, \dots, V_i, \dots, V_D)$ $(D = \sum_{i=1}^{d} \alpha_i)$ [30].

In the case of POPF computation, Liouville copula generates samples of correlated wind speeds by following procedures.

1) Denote

$$L_i = \alpha_1 + \alpha_2 + \cdots + \alpha_i, \quad (i = 1, \dots, d). \tag{10}$$

2) Let $\boldsymbol{W} = (W_1, \dots, W_i, \dots, W_d)$ be a d-dimension random vector, and

$$W_i = \sum_{k=L_{i-1}+1}^{L_i} \frac{-ln(V_k)}{S}, \quad (i = 1, \dots, d; \; L_0 = 0), \tag{11}$$

where S is a random variable with Gamma distribution, the PDF of S is

$$g(S) = \frac{1}{\Gamma(1/\theta)} S^{\frac{1}{\theta}-1} e^{-S}.$$

3) Transform $\boldsymbol{W}$ to $\boldsymbol{U}$ by

$$U_i = (1 + W_i)^{-\frac{1}{\theta}} \sum_{r=0}^{\alpha_i - 1} \frac{\Gamma\left(\frac{1}{\theta} + r\right)}{r! \cdot \theta \cdot \Gamma\left(\frac{1}{\theta} + 1\right)} \left(\frac{W_i}{1 + W_i}\right)^k, \quad (i = 1, 2, \dots, d), \tag{12}$$

where $\Gamma(\cdot)$ is the gamma function.

The above procedures can be represented by

$$\begin{pmatrix} V_1 \\ \vdots \\ V_i \\ \vdots \\ V_D \end{pmatrix} \xrightarrow{Eq.\ (11)} \begin{pmatrix} W_1 \\ \vdots \\ W_i \\ \vdots \\ W_d \end{pmatrix} \xrightarrow{Eq.\ (12)} \begin{pmatrix} U_1 \\ \vdots \\ U_i \\ \vdots \\ U_d \end{pmatrix}. \tag{13}$$

3.3 | Parameter estimation

When Liouville copula is used to fit correlated wind speeds, the dependence structure is characterized by parameters θ and α_i $(i=1,\dots,d)$. Here, a rank correlation matching method is proposed to specify parameters of Liouville copula.

Consider correlated wind speeds at two sites, which are denoted by X_i and X_j, respectively, denote Kendall's rank correlation coefficient between X_i and X_j as $\tau_{i,j}$, denote $(x_{s,i},\ x_{s,j})$ $(s=1,\dots,n)$ as samples of $(X_i,\ X_j)$, it has

$$\tau_{i,j} = \frac{2}{n(n-1)} \sum_{1\le s<h\le n} sgn(x_{s,i}-x_{h,i})sgn(x_{s,j}-x_{h,j}), \tag{14}$$

where $sgn(\cdot)$ is the sign function, $(x_{h,i},\ x_{h,j})$ is the hth sample of $(X_i,\ X_j)$.

On the other hand, $\tau_{i,j}$ can be obtained analytically by Liouville copula in terms of θ, α_i and α_j [30]

$$\tau_{i,j} = -1 + 4\sum_{r_i=0}^{\alpha_i-1}\sum_{r_j=0}^{\alpha_j-1} \frac{\Gamma\left(\frac{2}{\theta}\right)}{\left[\theta\cdot\Gamma\left(\frac{1}{\theta}+1\right)\right]^2}\cdot\frac{\Gamma(\alpha_i+\alpha_j+r_i+r_j)}{\Gamma(\alpha_i+\alpha_j)} \cdot\frac{B(\alpha_i+r_i,\alpha_j+r_j)\cdot B\left(\frac{1}{\theta}+r_i+r_j,\frac{1}{\theta}+\alpha_i+\alpha_j\right)}{B(\alpha_i,\alpha_j)r_i!r_j!}, \tag{15}$$

where $B(\cdot,\ \cdot)$ is beta function. By matching the correlation coefficient $\tau_{i,j}$ to that of wind speeds X_i and X_j, the parameters θ and α_i $(i=1,\dots,d)$ can be determined.

4 | LATTICE SAMPLING METHOD FOR POPF COMPUTATION

4.1 | Lattice sampling method

Let k and n be two integers, let '(k,n)' denote the greatest common divisor between k and n. For example,

$$(2,6)=2,\quad (5,6)=1.$$

Consider the reduced residue system (RRS) of n

$$\boldsymbol{K} = \{k|(k,n)=1,\ k=1,\dots,n\}, \tag{16}$$

where $\boldsymbol{K}$ comprises of integers from 1 to n that are relatively prime to n. The number of elements in $\boldsymbol{K}$ can be counted by using Euler's totient function $\varphi(n)$. For example, if $n=12$, $\boldsymbol{K}=\{1,5,7,11\}$, and $\varphi(12)=4$; if $n=15$, $\boldsymbol{K}=\{1,2,4,7,8,11,13,14\}$, and $\varphi(15)=8$.

Here, the RRS of n is used to construct a set of samples in a $\varphi(n)$-dimensional hypercube space $[0,1]^{\varphi(n)}$. Denote all elements in $\boldsymbol{K}$ as: "$k_1,\dots,k_i,\dots,k_{\varphi(n)}$", denote $\boldsymbol{v}_s=(v_{s,1},\dots,v_{s,i},\dots,v_{s,\varphi(n)})$ $(s=1,\dots,\varphi(n))$ as a set of samples,

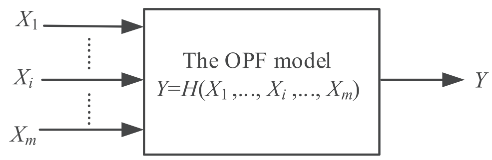

FIGURE 1 The probabilistic optimal power flow problem as a non-linear stochastic response problem.

and

$$t_{s,i} = \frac{[k_s\times k_i]_n}{n}, \qquad (s=1,\dots,\varphi(n)), \tag{17}$$

where $[\cdot]_n$ denotes the modulo operation. For example, $[5\times 7]_{12}=[35]_{12}=11$, $[2\times 11]_{15}=[22]_{15}=7$. Below are a set of samples developed from the RRS of $n=12$

$$\begin{pmatrix} \frac{1}{12} & \frac{5}{12} & \frac{7}{12} & \frac{11}{12} \\ \frac{5}{12} & \frac{1}{12} & \frac{11}{12} & \frac{7}{12} \\ \frac{7}{12} & \frac{11}{12} & \frac{1}{12} & \frac{5}{12} \\ \frac{11}{12} & \frac{7}{12} & \frac{5}{12} & \frac{1}{12} \end{pmatrix}.$$

The RRS of n has the following property: 'if $k_i\neq k_j$, then, $[k_s\times k_i]_n \neq [k_s\times k_j]_n$'. This property enures that the low discrepancy sequences from Equation (17) can avoid clumping together and uniformly spread across the sampling space. In conjunction with the generalized Johnson system and Liouville copula, this lattice sampling technique can well represent statistical features of wind speeds.

4.2 | POPF computation

Mathematically, the POPF problem can be formulated as a non-linear stochastic response problem, which is illustrated by Figure 1, where $\boldsymbol{X}=(X_1,\dots,X_i,\dots,X_m)$ denotes all random variables in the OPF model, Y denotes an arbitrary OPF solution.

The aim of POPF computation is to calculate statistical information of Y from those of X_i $(i=1,\dots,m)$

$$Y = H(\boldsymbol{X}),\ \ \boldsymbol{X}=(X_1,\dots,X_i,\dots,X_m), \tag{18}$$

where X_i $(i=1,\dots,m)$ are POPF inputs, Y is POPF outputs, the implicit function $H(\cdot)$ is defined by OPF model.

Via the quantile function of X_i in Equation (5) and Liouville copula in Equation (13), the POPF inputs $\boldsymbol{X}$ can be related to an M-dimensional independent uniform vector $\boldsymbol{V}=(V_1,\dots,V_i,\dots,V_M)$

$$Y = H(\boldsymbol{X}) = G(V_1,\dots,V_i,\dots,V_M). \tag{19}$$

According to Equation (19), statistical moments of the POPF outputs Y can be obtained by lattice sampling method

$$E[Y^r] \simeq \frac{1}{\varphi(n)} \sum_{s=1}^{\varphi(n)} y_s^r = \frac{1}{\varphi(n)} \sum_{s=1}^{\varphi(n)} G^r(\boldsymbol{t}_s), \tag{20}$$

where $\boldsymbol{v}_s = (v_{s,1}, \ldots, v_{s,j}, \ldots, v_{s,M})$ $(s = 1, \ldots, \varphi(n))$ are samples generated by Equation (17), and n is an integer with $\varphi(n) \geq M$.

By using samples of Y, the distribution functions of Y can be also be reconstructed. Here, a LMM is proposed to recover the CDF of POPF outputs

$$F(Y) = \frac{1}{N} \sum_{k=1}^{N} \Psi(Y, \mu_k, \sigma_k) = \frac{1}{N} \sum_{k=1}^{N} \left(1 + e^{-\frac{Y-\mu_k}{\sigma_k}}\right)^{-1}, \tag{21}$$

where N is the number of mixture components, $\Psi(Y, \mu_k, \sigma_k)$ is the CDF of a logistic random variable, μ_k and σ_k are parameters of the kth component respectively $(k = 1, \ldots, N)$.

Denote all $2N$ parameters of LMM as a vector

$$\begin{aligned} \boldsymbol{x} &= (\mu_1, \ldots, \mu_k, \ldots, \mu_N, \sigma_1, \ldots, \sigma_k, \ldots, \sigma_N)^T \\ &= (x_1, \ldots, x_k, \ldots, x_{2N})^T. \end{aligned}$$

Denote

$$g(\boldsymbol{x}, u_i) = \left(\frac{1}{N} \sum_{k=1}^{N} \frac{1}{1 + e^{-\frac{y_i - \mu_k}{\sigma_k}}} \right) - u_i, \quad (i = 1, \ldots, L;\ L \geq 2N), \tag{22}$$

where y_i is a sample of POPF outputs Y, u_i is the corresponding percentage value of y_i $(i = 1, \ldots, L;\ L > 2N)$.

Here, Levenberg–Marquardt (LM) algorithm is employed to specify the parameter vector $\boldsymbol{x}$, which is obtained by the following iterative formula

$$\begin{aligned} \boldsymbol{x}_{k+1} &= \boldsymbol{x}_k + \left(\boldsymbol{J}^T\boldsymbol{J} + \lambda \cdot \boldsymbol{\Lambda}\right) \backslash \left(\boldsymbol{J}^T\boldsymbol{G}\right), \qquad (\lambda > 0) \\ \boldsymbol{G} &= -\left(g(\boldsymbol{x}_k, u_1), \ldots, g(\boldsymbol{x}_k, u_i), \ldots, g(\boldsymbol{x}_k, u_L)\right)^T, \end{aligned} \tag{23}$$

where '\' denotes the matrix left division operation, $\boldsymbol{J}$ is the Jacobian matrix of Equation (22): $\boldsymbol{J} = \{\frac{\partial g(\boldsymbol{x}, u_i)}{\partial x_k}\}$ $(i = 1, \ldots, L;$ $k = 1, \ldots, 2N)$, λ is the damping factor, $\boldsymbol{\Lambda}$ is a diagonal matrix of size $(2N) \times (2N)$, which consists of diagonal elements of $\boldsymbol{J}^T\boldsymbol{J}$. In Equation (23), the initial guess $\boldsymbol{x}_0$ for $\boldsymbol{x}$ is generated by uniform deviates with in [0, 1].

4.3 | Computational procedure

Below are procedures of the proposed POPF computation algorithms, which are also depicted in Figure 2.

1) Let $\boldsymbol{X} = (X_1, \ldots, X_i, \ldots, X_m)$ denote all POPF inputs, fit distributions to X_i by the generalized Johnson system in Section 2, construct the quantile function of X_i by Equation (5) $(i = 1, \ldots, m)$.
2) Calculate Kendall's rank correlation coefficient $\tau_{i,j}$ of POPF inputs by Equation (14) $(i, j = 1, \ldots, m)$, estimate parameters of Liouville copula by Equation (15).
3) Generate samples $\boldsymbol{v}_k = (v_{s,1}, \ldots, v_{s,j}, \ldots, v_{s,M})$ $(s = 1, \ldots, \varphi(n))$ by Equation (17), transform them to correlated standard uniform deviates by Equation (13), which are further transformed to samples of POPF inputs $\boldsymbol{x}_s = (x_{s,1}, \ldots, x_{s,i}, \ldots, x_{s,m})$ by Equation (5)

$$x_{s,i} = F_i^{-1}(u_{s,i}), \quad (s = 1, \ldots, \varphi(n);\ i = 1, \ldots, m).$$

4) Perform deterministic OPF calculations to generate samples of POPF outputs, calculate moments of POPF outputs, and recover distribution functions of POPF outputs by LMM in Equation (21).

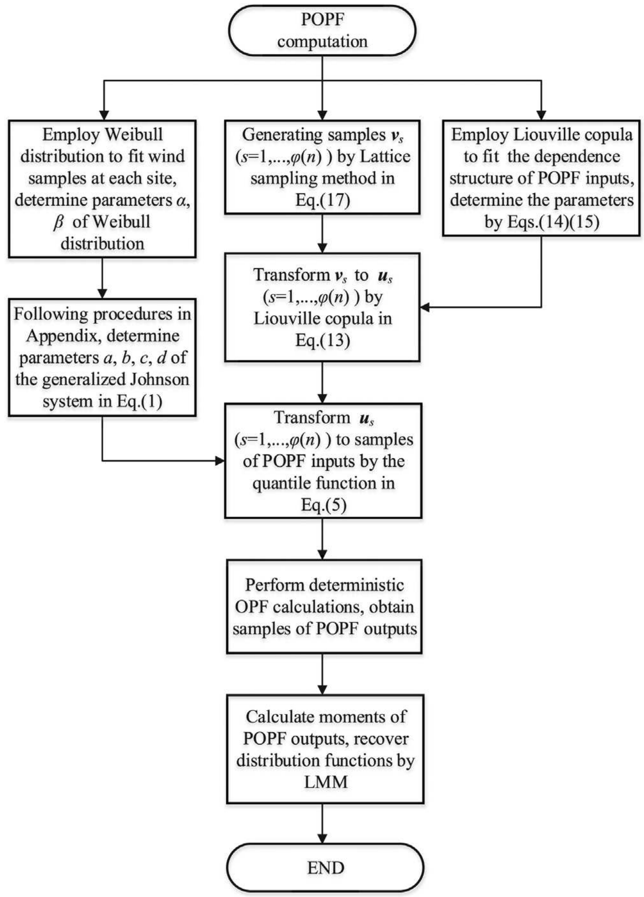

FIGURE 2 The flowchart of the proposed probabilistic optimal power flow computation algorithm.

5 | CASE STUDY

5.1 | Fitting marginal distributions of wind samples

When the copula method is employed to characterize statistical features of correlated wind speeds, marginal distributions

TABLE 2 The parameters of the generalized Johnson system and Johnson system.

Sample	Model	α	β	a	b	c	d
I	S_B	–	–	−0.7936	14.4403	−0.3610	0.9421
	W_B	8.4746	2.6045	−5.0667	19.6570	−2.6144	3.9043
II	S_B	–	–	−0.3211	20.5606	1.2567	1.2719
	W_B	6.5876	2.0180	−2.9466	22.2339	2.2858	4.9736
III	S_B	–	–	2.2237	11.5010	−2.4457	5.4132
	W_B	8.4877	3.7056	5.2921	7.0090	−2.4118	7.5115

should be provided. In Table A1 of Appendix, a generalized Johnson system based on Weibull distribution is presented to recover the CDF, PDF and quantile function of wind samples. In order to avoid ambiguity, the three models derived from Weibull distribution are, respectively, denoted as W_U, W_L and W_B. When the Johnson system based on Weibull distribution is used to fit wind samples, it first employs Weibull distribution to fit wind samples, where the parameters α and β are determined by the maximum likelihood method, then it employs the percentile matching method in Appendix to select an appropriate model and to specify values of a, b, c and d.

Here, three sets of wind samples are taken from three wind farms in Northwest China, which are denoted as Sample-I, Sample-II and Sample-III, respectively. Except for the proposed generalized Johnson system, Weibull distribution and the original Johnson system based on standard normal distribution are also employed to fit wind samples, the PDFs are depicted in Figure 3, the parameters are summarized in Table 2. In order to demonstrate the accuracy of these three models, the percentage of each wind speed sample is calculated by the fitted theoretical distribution and empirical distribution, respectively, and the absolute error is calculated

$$\varepsilon_k = \left| F(x_k) - F_e(x_k) \right| \times 100[\%], \quad (k = 1, \ldots, n), \tag{24}$$

where x_k denotes the kth wind speed sample, $F(\cdot)$ is the CDF established by Weibull distribution, the original Johnson system or the generalized Johnson system, $F_e(\cdot)$ is the empirical CDF given by wind speed data. The minimum, average and maximum values of ε_k $(k = 1, \ldots, n)$ are presented in Table 3.

As shown in Table 3 and Figure 3, because the Johnson S_B model has four parameters to represent statistical features of wind samples, it behaves better than the two-parameter Weibull distribution. In comparison to the S_B model, the proposed W_B model has six parameters to include statistical information of the target wind data, and thus yields an even better fitting. As noted in Section 2, Weibull distribution is more accurate than normal distribution for modelling the uncertainty of wind speed, therefore, the generalized Johnson system based on Weibull distribution performs better than the original Johnson system based on normal distribution. It is worth mentioning that if there is a more appropriate distribution function $\Psi(\cdot)$ for characterizing wind speed, a new generalized Johnson system can be developed to fit wind samples by procedures in Section 2.

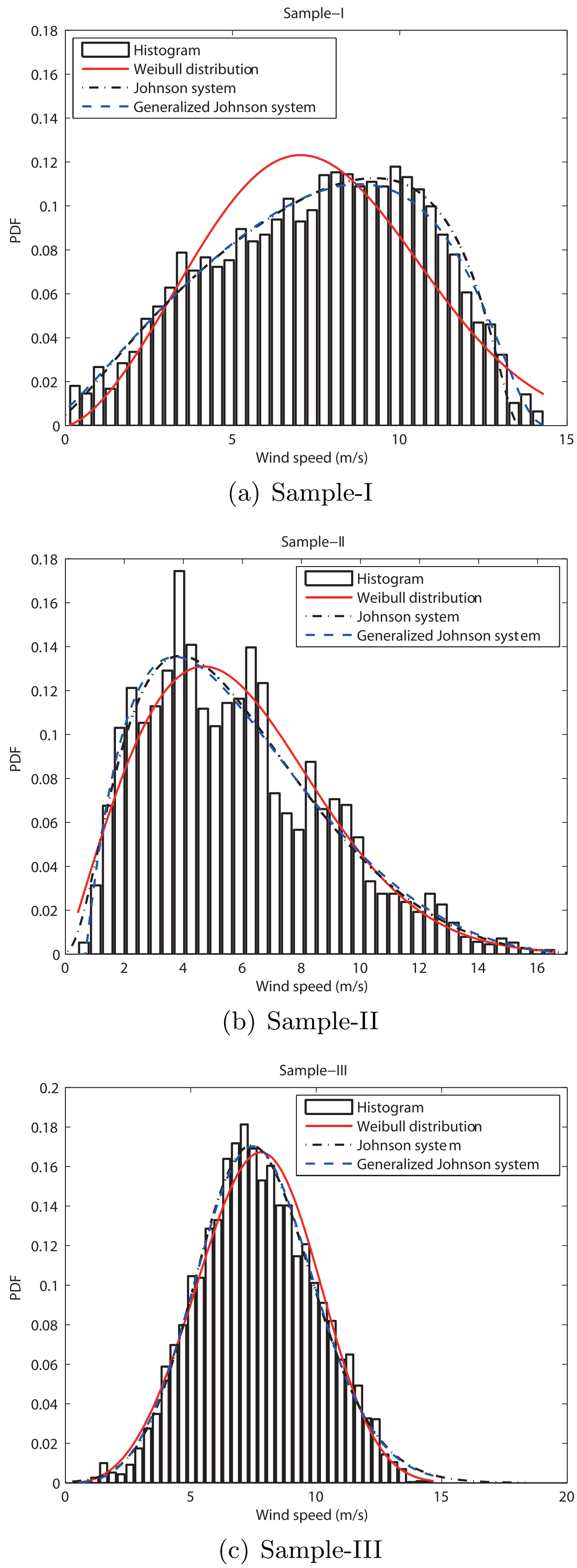

(a) Sample-I

(b) Sample-II

(c) Sample-III

FIGURE 3 The probability density functions of wind speeds.

TABLE 3 The absolute errors in % between theoretical cumulative distribution function (CDF) and empirical CDF.

Sample	Model	Minimum	Average	Maximum
	Weibull	1.01×10^{-6}	3.12	5.84
I	S_B	3.55×10^{-5}	1.05	1.63
	W_B	1.41×10^{-5}	0.47	1.14
	Weibull	5.15×10^{-5}	1.33	3.71
II	S_B	1.83×10^{-5}	0.94	2.16
	W_B	8.74×10^{-7}	0.52	1.31
	Weibull	7.95×10^{-4}	0.84	2.33
III	S_B	6.03×10^{-4}	0.57	1.82
	W_B	7.12×10^{-5}	0.31	0.94

5.2 | Fitting correlated wind speed data

Here, except for Liouville copula in Section 3, Archimedean copula based on Clayton generator in Equation (9) is also employed to match the correlation structure of wind speeds

$$\boldsymbol{C}_3(U_1,U_2,U_3)=\left[U_1^{-\theta_1}+\left(U_2^{-\theta_2}+U_3^{-\theta_2}-1\right)^{\theta_1/\theta_2}-1\right]^{-1/\theta_1}, \tag{25}$$

and Kendall's τ of Archimedean copula in Equation (25) is

$$\tau=\frac{\theta}{\theta+2}. \tag{26}$$

If θ_1 is equal to θ_2, that is, $\theta_1=\theta_2$, $\boldsymbol{C}_3(U_1,U_2,U_3)$ in Equation (25) reduces to the exchangeable Archimedean (EA) copula; if $\theta_1\neq\theta_2$, $\boldsymbol{C}_3(U_1,U_2,U_3)$ would be the nested Archimedean (NA) copula.

For wind samples in Figure 3, if Kendall's τ is employed to measure the dependence structure, the following correlation matrix can be obtained by Equation (14)

$$\boldsymbol{R_X}=\begin{pmatrix}1 & 0.442 & 0.458\\ 0.442 & 1 & 0.745\\ 0.458 & 0.745 & 1\end{pmatrix}.$$

TABLE 5 The absolute error in % between copula models and empirical joint cumulative distribution function.

	Minimum	Average	Maximum
EA	2.21×10^{-4}	3.52	10.2
NA	9.23×10^{-5}	1.88	4.74
Liouville	1.52×10^{-5}	0.59	1.25

By matching the correlation matrix of copula to $\boldsymbol{R_X}$, the parameters of copula can be obtained, which are presented in Table 4. One point worth noting is that Liouville copula and Archimedean copula in Equation (25) are both constructed by Clayton generator, but Liouville copula has four parameters to control the dependence structure, and thus is more flexible. As shown in Table 4, the Liouville copula yields a more accurate match to the correlation matrix of wind speeds.

According to Equation (7), the joint CDF of wind speeds can be recovered

$$\boldsymbol{F}_3(\boldsymbol{X})=\boldsymbol{C}_3\left[F_1(X_1),F_2(X_2),\dots,F_3(X_3)\right], \tag{27}$$

where $\boldsymbol{C}_3(\cdot)$ is the copula model, $F_i(X_i)$ $(i=1,2,3)$ are marginal CDFs of wind speeds, which can be obtained by the generalized Johnson system in Equation (2) and Table A1. Here, the following error index is defined to measure the performance of copulas in Table 4

$$\varepsilon_k=\left|\boldsymbol{F}_3(\boldsymbol{x}_k)-\widehat{\boldsymbol{F}}_3(\boldsymbol{x}_k)\right|\times100[\%]\quad(k=1,\dots,n), \tag{28}$$

where $\boldsymbol{x}_k=(x_{k,1},x_{k,2},x_{k,3})$ denotes the kth sample of wind speeds, $F(\boldsymbol{x}_k)$ is the percentage evaluated by $\boldsymbol{F}_3(\cdot)$ in Equation (27), $\widehat{\boldsymbol{F}}_3(\boldsymbol{x}_k)$ is the corresponding one given by the empirical joint CDF, Table 5 summarizes the minimum, average and maximum values of ε_k $(k=1,\dots,n)$. As can be seen, the joint CDF constructed by Liouville copula is more accurate than those based on EA copula and NA copula.

In comparison to EA copula, the NA copula has two different parameters θ_1 and θ_2 to regulate the dependence structure, and performs better in characterizing statistical features of wind speeds. In the case of Liouville copula, it employs 30 random variables to represent the dependence structure of wind speeds (see Equation (13) and Table 4: $\alpha_1+\alpha_2+\alpha_3=30$),

TABLE 4 The parameters and correlation matrix of Archimedean copula and Liouville copula.

Copula	Parameters	Correlation matrix	Absolute error
EA	$\theta_1=\theta_2=2.425$	$\begin{pmatrix}1 & 0.548 & 0.548\\ 0.548 & 1 & 0.548\\ 0.548 & 0.548 & 1\end{pmatrix}$	$\begin{pmatrix}0 & 0.106 & 0.090\\ 0.106 & 0 & 0.197\\ 0.090 & 0.197 & 0\end{pmatrix}$
NA	$\theta_1=1.636$ $\theta_2=5.843$	$\begin{pmatrix}1 & 0.450 & 0.450\\ 0.450 & 1 & 0.745\\ 0.450 & 0.745 & 1\end{pmatrix}$	$\begin{pmatrix}0 & 0.008 & 0.008\\ 0.008 & 0 & 0\\ 0.008 & 0 & 0\end{pmatrix}$
Liouville	$\theta=0.871,\ \alpha_1=1$ $\alpha_2=8,\ \alpha_3=18$	$\begin{pmatrix}1 & 0.442 & 0.459\\ 0.442 & 1 & 0.745\\ 0.459 & 0.745 & 1\end{pmatrix}$	$\begin{pmatrix}0 & 0 & 0.001\\ 0 & 0 & 0\\ 0.001 & 0 & 0\end{pmatrix}$

TABLE 6 Wind turbines included in IEEE 118-bus system.

Nodes	Number of turbines	Wind speed
2, 13, 44, 52, 83	20	X_1
3, 14, 48, 53, 84	20	X_2
5, 16, 50, 82, 86	20	X_3

whereby the statistical information of wind samples can be precisely described. Figure 4 depicts the pairwise scatter plots of wind samples in the uniform space $[0,\ 1]^2$, where it can be seen that the scatter plots of $(U_1,\ U_2)$ and $(U_1,\ U_3)$ exhibit strong asymmetry.

With the algorithms in reference [30, 31], it generates 6550 samples for each copula model in Table 4, the pairwise scatter plots are also shown in Figure 4. Because EA copula can only model the homogeneous dependence structure, leading to that dependence structures between arbitrary two wind speeds are the same. The NA copula is capable of modelling the heterogeneous dependence structure, the scatter plot of $(U_2,\ U_3)$ is different to those of $(U_1,\ U_2)$ and $(U_1,\ U_3)$, which accounts for its better performance than EA copula (see Tables 3 and 5). However, due to the limited flexibility, the EA copula and NA copula fail to capture the asymmetry of dependence structures of $(U_1,\ U_2)$ and $(U_1,\ U_3)$, and they show lower accuracy than Liouville copula.

5.3 | POPF computation considering correlated wind speeds

Consider IEEE 118-bus system with 15 nodes integrated with wind turbines [32], which are shown in Table 6.

Let P denote the wind turbine output power, and

$$P = \begin{cases} \frac{2X_i - 8}{11} & 4 \le X_i \le 15 \\ 2 & 15 < X_i \le 25 \quad (MW), \\ 0 & \text{else} \end{cases} \tag{29}$$

where X_i $(i = 1, 2, 3)$ are wind speeds. Wind turbines are double-fed induction generators, and their reactive power is compensated by the controller, keeping the constant value unchanged, usually very close to zero.

By using the generalized Johnson system in Table 2 and Liouville copula in Table 4, the uncertainty of wind speeds is represented by 27 independent standard uniform variable. For the tested IEEE 118-bus system, load demands are assumed to follow normal distributions, where mean values are base case data, standard deviations are 5% of mean values and the correlation coefficients among load demands are 0.5. Hence, the number of POPF inputs is 126, and the value of M in Equation (19) is 126. Table 7 presents three different values of n and corresponding values of $\varphi(n)$ in Equation (20).

Except for lattice sampling method, Sobol sequence and LHS are also used for POPF computation. The program has been run in MATLAB on a 2.3 GHz Intel Corei3-2350M computer with 3 GB of RAM. The objective function of deterministic OPF model is to maximize social welfare, the interior-point method is employed to solve the deterministic OPF model [33]. The following error index is defined to measure the performance of the employed algorithms

TABLE 7 The values of n and $\varphi(n)$.

n	262	1250	3750
$\varphi(n)$	130	500	1000

$$\bar{\varepsilon}_r = \frac{1}{N}\sum_{j=1}^{N}\left|\frac{m_{r,j}^{\mathrm{MCS}} - m_{r,j}^{*}}{m_{r,j}^{MCS}}\right| \times 100[\%], \tag{30}$$

where $m_{r,j}^{\mathrm{MCS}}$ is the mean $(r = 1)$ or standard deviation $(r = 2)$ of jth POPF outputs from MCS with 10^5 trials, $\mu_{r,j}^{*}$ is the one estimated by Sobol sequence, LHS or lattice sampling method. $\bar{\varepsilon}_r$ is the average absolute relative error. N is the number of the output variables in the system.

Table 8 summarizes results of Sobol sequence, LHS and lattice sampling method, where V, Θ, Pl and Ql denote the voltage, phase angle, active power flow and reactive power flow, respectively. As shown in Table 8, all three algorithms can yield accurate estimates for mean values; but in the case of calculating standard deviations of POPF outputs, Sobol sequence performs poorer than LHS and lattice sampling method, and the proposed lattice sampling method is more accurate than LHS, the results of Lattice sampling method with 500 points are comparable to those of LHS with 1000 points. Hence, when lattice sampling method is used for POPF computation, it can alleviate the computational burden significantly.

With the obtained samples, the distribution functions of POPF outputs can be recovered. According to Equation (21), the PDF of POPF outputs is

$$f(Y) = \frac{d[F(Y)]}{dY} = \frac{1}{N}\sum_{k=1}^{N}\frac{1}{\sigma_k}\cdot e^{-\frac{Y-\mu_k}{\sigma_k}}\cdot\left(1 + e^{-\frac{Y-\mu_k}{\sigma_k}}\right)^{-2}. \tag{31}$$

Here, LMM in Equation (31) is used to fit PDFs of the reactive power flows of line 16–17 and line 85–86, which are denoted as Ql_{16-17} and Ql_{85-86}, respectively. Except for LMM in Equation (31), GMM is also employed to fit PDFs of Ql_{16-17} and Ql_{85-86}

$$f(Y) = \frac{1}{N}\sum_{k=1}^{N}\phi(y, \mu_k, \sigma_k) = \frac{1}{N}\sum_{k=1}^{N}\frac{1}{\sqrt{2\pi}}e^{-\frac{(Y-\mu_k)^2}{2\sigma_k^2}}. \tag{32}$$

Following the procedures in Section 4.2, the parameters of LMM and GMM are determined and given in Table 9, the PDFs are plotted in Figure 5. An inspection of Figure 5 demonstrates that both LMM and GMM can accurately fit the histogram of Ql_{16-17}, but in the case of Ql_{85-86}, the tails of the histogram are

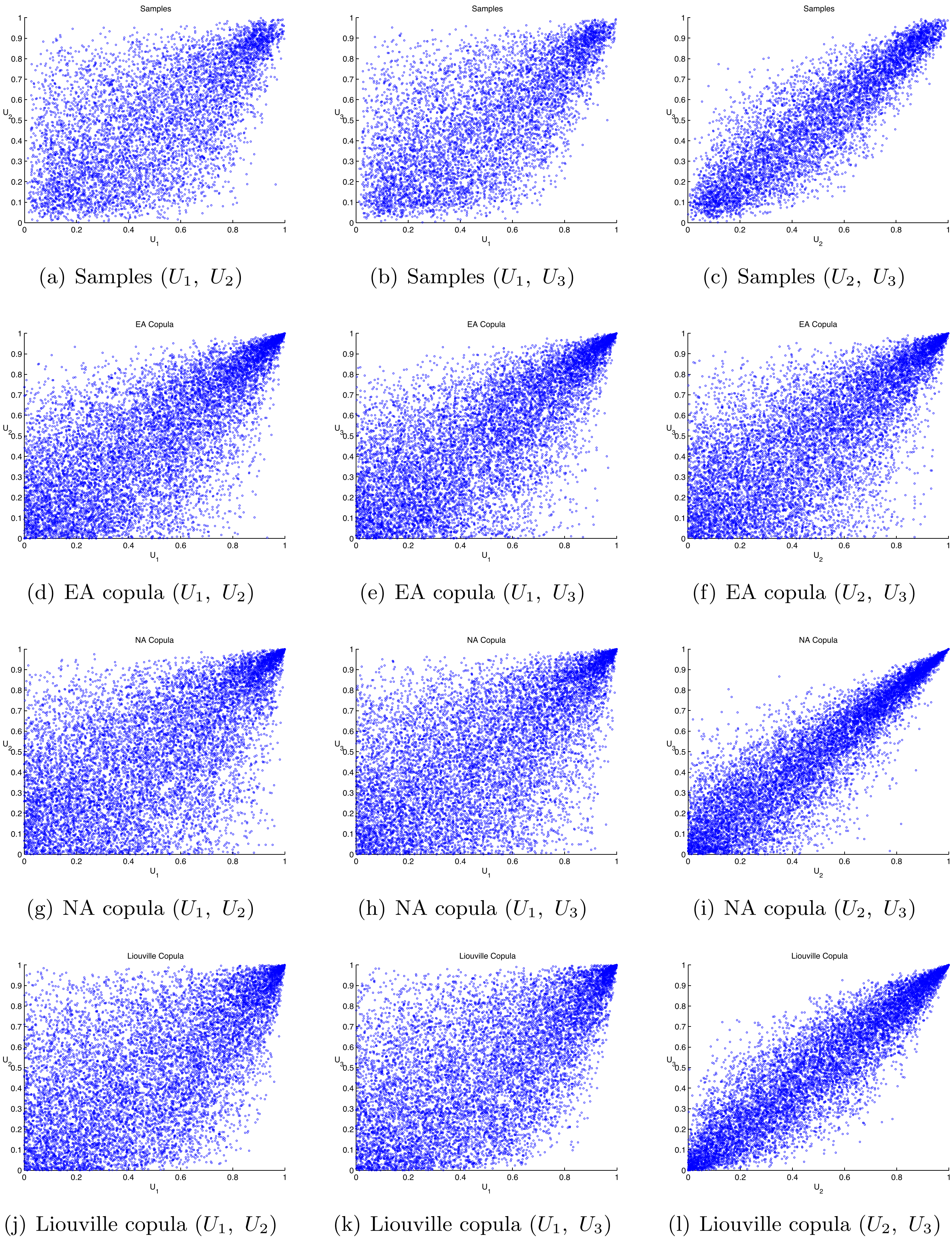

FIGURE 4 The scatter plots of wind speed samples and copulas.

TABLE 8 Error in % of Sobol sequence, Latin hypercube sampling and lattice sampling method.

		130 points			500 points			1000 points		
		Sobol	**LHS**	**Lattice**	**Sobol**	**LHS**	**Lattice**	**Sobol**	**LHS**	**Lattice**
V	$\bar{\varepsilon}_1$	0.004	0.001	0.001	0.002	0.001	0.001	0.002	0.001	0.002
	$\bar{\varepsilon}_2$	6.19	2.66	2.53	4.04	1.91	1.33	3.70	1.80	0.85
Θ	$\bar{\varepsilon}_1$	0.24	0.74	0.15	0.13	0.29	0.17	0.09	0.19	0.11
	$\bar{\varepsilon}_2$	9.72	4.54	2.30	5.67	2.43	1.81	4.22	2.06	1.36
Pl	$\bar{\varepsilon}_1$	0.73	0.77	0.26	0.38	0.26	0.23	0.25	0.23	0.17
	$\bar{\varepsilon}_2$	8.13	3.63	3.58	4.88	2.23	1.87	4.03	1.70	1.33
Ql	$\bar{\varepsilon}_1$	1.14	0.59	0.49	0.74	0.24	0.22	0.61	0.21	0.11
	$\bar{\varepsilon}_2$	9.50	4.38	4.11	5.84	2.17	1.79	4.21	1.94	1.21
Time (s)			148.6			571.7			1143.4	

TABLE 9 The parameters of logistic mixture model and Gaussian mixture model.

Ql_{16-17}				Ql_{85-86}			
LMM		**GMM**		**LMM**		**GMM**	
μ_k	σ_k	μ_k	σ_k	μ_k	σ_k	μ_k	σ_k
−0.08431	0.00224	−0.08447	0.01166	0.01785	0.00198	0.00572	0.01086
−0.09534	0.00222	−0.07617	0.00798	0.00395	0.00246	0.00894	0.01215
−0.10903	0.00687	−0.09056	0.01679	−0.00543	0.00224	0.02712	0.00368
−0.07678	0.00262	−0.08316	0.01029	0.02343	0.00225	0.00774	0.01172
−0.09035	0.00199	−0.09207	0.00397	0.01114	0.00209	0.01997	0.00435
−0.06921	0.00401	−0.09871	0.02053	0.02782	0.00244	0.00818	0.01189

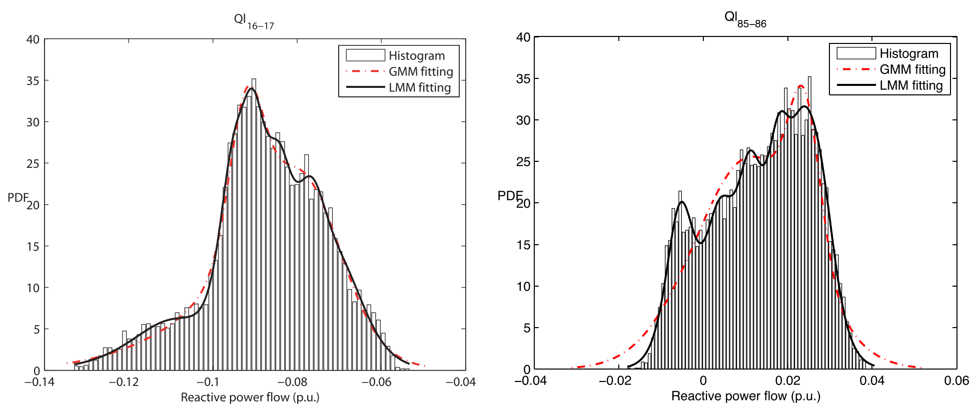

(a) Ql_{16-17} (b) Ql_{85-86}

FIGURE 5 The probability density functions of reactive power flows.

not well modelled by GMM. Testing for various POPF outputs, it is found that if the shape of histogram is unimodal, both models can accurately recover the PDF of target samples of POPF outputs; but if the PDF shape is multimodal, LMM performs better than GMM.

6 | CONCLUSION

This paper develops a lattice sampling technique-based POPF to assess the influence of correlated wind speeds on power grid, the conclusions are as follows:

1) The Johnson system can be extended to non-normal variables with zero mean, the parameters can be specified by the percentile matching method; because the Johnson system based on Weibull distribution has six parameters to capture statistical information of wind speeds, it performs better for fitting wind samples than the original four-parameter Johnson system based on standard normal distribution.
2) In practical settings, it is possible that the dependence structure of wind speeds is asymmetric, the elliptical copula and Archimedean copula fail to capture such asymmetry, and Liouville copula serves as a useful tool to handle asymmetric dependency of wind speeds.
3) Sobol sequence, LHS and the proposed Lattice sampling method are low discrepancy sequences, the simulation on IEEE 118-bus indicate that lattice sampling method is more efficient and accurate in POPF computation.

AUTHOR CONTRIBUTIONS

Qing Xiao: Conceptualization; data curation; funding acquisition; methodology; writing—original draft. **Zhuangxi Tan**: Methodology; software; writing—original draft; writing—review and editing. **Min Du**: Conceptualization; software; validation; writing—review and editing.

ACKNOWLEDGEMENTS

This work was supported by National Natural Science Foundation of China (12271155) and Doctoral Research Start-up Fund of Hunan University of Science and Technology (E52170).

CONFLICT OF INTEREST STATEMENT

The authors declare no conflicts of interests.

DATA AVAILABILITY STATEMENT

The data that support the findings of this study are available on request from the corresponding author.

ORCID

Qing Xiao https://orcid.org/0000-0002-7386-3793

REFERENCES

1. Hassan, M.H., Daqaq, F., Kamel, S., Hussien, A.G., Zawbaa, H.M.: An enhanced hunter-prey optimization for optimal power flow with FACTS devices and wind power integration. IET Gener. Transm. Distrib. 17(14), 3115–3139 (2023)
2. Mohamed, A.A., Kamel, S., Hassan, M.H., Zeinoddini-Meymand, H.: CAVOA: A chaotic optimization algorithm for optimal power flow with facts devices and stochastic wind power generation. IET Gener. Transm. Distrib. 18(1), 121–144 (2024)
3. Ullah, Z., Wang, S., Wu, G., Hasanien, H.M., Jabbar, M.W., Qazi, H.S., et al.: Advanced studies for probabilistic optimal power flow in active distribution networks: A scientometric review. IET Gener. Transm. Distrib. 16(18), 3579–3604 (2022)
4. Xie, K., Li, Y., Li, W.: Modelling wind speed dependence in system reliability assessment using copulas. IET Renewable Power Gener. 6(6), 392–399 (2012)
5. Louie, H.: Evaluation of bivariate Archimedean and elliptical copulas to model wind power dependency structures. Wind Energy 17(2), 225–240 (2014)
6. Roy, R., Jadhav, H.: Optimal power flow solution of power system incorporating stochastic wind power using gbest guided artificial bee colony algorithm. Int. J. Electr. Power Energy Syst. 64, 562–578 (2015)
7. Jadhav, H., Roy, R.: Stochastic optimal power flow incorporating offshore wind farm and electric vehicles. Int. J. Electr. Power Energy Syst. 69, 173–187 (2015)
8. Li, Y., Li, W., Yan, W., Yu, J., Zhao, X.: Probabilistic optimal power flow considering correlations of wind speeds following different distributions. IEEE Trans. Power Syst. 29(4), 1847–1854 (2014)
9. Xiao, Q., Zhou, S.: Probabilistic power flow computation considering correlated wind speeds. Appl. Energy 231, 677–685 (2018)
10. Xiao, Q.: Modeling uncertainties in power system by generalized lambda distribution. Int. J. Emerging Electr. Power Syst. 15(3), 195–203 (2014)
11. Xiao, Q., Zhou, S., Wu, L., Zhao, Y., Zhou, Y.: Investigating univariate dimension reduction model for probabilistic power flow computation. Electr. Power Compon. Syst. 47(6-7), 561–572 (2019)
12. Ruiz-Rodriguez, F., Hernandez, J., Jurado, F.: Probabilistic load flow for photovoltaic distributed generation using the Cornish–Fisher expansion. Electr. Power Syst. Res. 89, 129–138 (2012)
13. Zou, B., Xiao, Q.: Solving probabilistic optimal power flow problem using quasi Monte Carlo method and ninth-order polynomial normal transformation. IEEE Trans. Power Syst. 29(1), 300–306 (2014)
14. Zhou, S., Xiao, Q., Wu, L.: Probabilistic power flow analysis with correlated wind speeds. Renew. Energy 145, 2169–2177 (2020)
15. Le, D.D., Nguyen, N.T.A., Van Duong, N., Berizzi, A.: Advanced probabilistic power flow methodology for power systems with renewable resources. Turk. J. Elec. Eng. Comp. Sci. 25(2), 1154–1162 (2017)
16. Xiao, Q., Zhou, S., Xiao, H.: Probabilistic optimal power flow analysis incorporating correlated wind sources. Int. Trans. Electr. Energy Syst. 30(8), 12441 (2020)
17. Cao, J., Yan, Z.: Probabilistic optimal power flow considering dependences of wind speed among wind farms by pair-copula method. Int. J. Electr. Power Energy Syst. 84, 296–307 (2017)
18. Li, G., Lu, W., Bian, J., Qin, F., Wu, J.: Probabilistic optimal power flow calculation method based on adaptive diffusion kernel density estimation. Front. Energy Res. 7(128), 1–10 (2019)
19. Cui, M., Feng, C., Wang, Z., Zhang, J.: Statistical representation of wind power ramps using a generalized Gaussian mixture model. IEEE Trans. Sustainable Energy 9(1), 261–272 (2018)
20. Ke, D., Chung, C., Sun, Y.: A novel probabilistic optimal power flow model with uncertain wind power generation described by customized Gaussian mixture model. IEEE Trans. Sustainable Energy 7(1), 200–212 (2016)
21. Xiao, Q., Zhou, S.: Matching a correlation coefficient by a Gaussian copula. Commun. Stat.-Theory Methods 48(7), 1728–1747 (2019)
22. Xie, Z., Ji, T., Li, M., Wu, Q.: Quasi-Monte Carlo based probabilistic optimal power flow considering the correlation of wind speeds using copula function. IEEE Trans. Power Syst. 33(2), 2239–2247 (2018)
23. Li, Y., Xie, K., Hu, B.: Copula-ARMA model for multivariate wind speed and its applications in reliability assessment of generating systems. J. Electr. Eng. Technol. 8(3), 421–427 (2013)
24. Tamtum, A., Schellenberg, A., Rosehart, W.D.: Enhancements to the cumulant method for probabilistic optimal power flow studies. IEEE Trans. Power Syst. 24(4), 1739–1746 (2009)
25. Alavi, S.A., Ahmadian, A., Aliakbar-Golkar, M.: Optimal probabilistic energy management in a typical micro-grid based-on robust optimization and point estimate method. Energy Convers. Manage. 95, 314–325 (2015)
26. Shargh, S., Mohammadi-Ivatloo, B., Seyedi, H., Abapour, M., et al.: Probabilistic multi-objective optimal power flow considering correlated wind power and load uncertainties. Renew. Energy 94, 10–21 (2016)
27. Aien, M., Fotuhi-Firuzabad, M., Aminifar, F.: Unscented transformation-based probabilistic optimal power flow for modeling the effect of wind power generation. Turk. J. Elec. Eng. Comp. Sci. 21(5), 1284–1301 (2013)
28. Xiao, Q., Zhou, S.: Comparing unscented transformation and point estimate method for probabilistic power flow computation. COMPEL Int. J. Comput. Math. Electr. Electron. Eng. 37(3), 1290–1303 (2018)
29. Hill, I.D., Hill, R., Holder, R.L.: Fitting Johnson curves by moments. J. R. Stat. Soc. Ser. C-App. Stat. 25(2), 180–189 (1976)
30. McNeil, A.J., Nešlehová, J.: From Archimedean to Liouville copulas. J. Multivariate Anal. 101(8), 1772–1790 (2010)

31. Hofert, M.: Efficiently sampling nested Archimedean copulas. Comput. Stat. Data Anal. 55(1), 57–70 (2011)
32. Usaola, J.: Probabilistic load flow with correlated wind power injections. Electr. Power Syst. Res. 80(5), 528–536 (2010)
33. Milano, F.: An open source power system analysis toolbox. IEEE Trans. Power Syst. 20(3), 1199–1206 (2005)

How to cite this article: Xiao, Q., Tan, Z., Du, M.: Probabilistic optimal power flow computation for power grid including correlated wind sources. IET Gener. Transm. Distrib. 1–14 (2024). https://doi.org/10.1049/gtd2.13196

APPENDIX

The parameters of the generalized Johnson system can be determined by following procedures.

1) Denote $x_1, \dots, x_k, \dots, x_n$ as a set of wind speed samples, denote the empirical quantile function as $F_e^{-1}(\cdot)$. Select a real number θ, and compute the following quantiles

$$x_{-3\theta} = F_e^{-1}[\Psi(-3\theta)],\ \ x_{-\theta} = F_e^{-1}[\Psi(-\theta)],$$
$$x_{3\theta} = F_e^{-1}[\Psi(3\theta)],\quad x_{\theta} = F_e^{-1}[\Psi(\theta)]. \tag{A1}$$

2) Denote

$$A = x_3 - x_1,\ \ B = x_{-1} - x_{-3},\ \ C = x_1 - x_{-1}. \tag{A2}$$

3) If $\frac{AB}{C^2} > 1$, the S_U (W_U) distribution should be employed, and the parameters can be calculated as:

$$a = \frac{x_1 + x_{-1}}{2} + \frac{B - A}{2(A + B - 2C)},$$
$$b = \frac{2C\sqrt{AB - C^2}}{(A + B - 2C)\sqrt{A/C + B/C + 2}},$$
$$c = d \cdot sinh^{-1}\left(\frac{B - A}{2\sqrt{AB - C^2}}\right),\ \ d = \frac{2}{cosh^{-1}\left(\frac{A + B}{2C}\right)}. \tag{A3}$$

If $\frac{AB}{C^2} = 1$, the S_L (W_L) distribution should be employed, and the parameters are

$$a = \frac{x_1 + x_{-1}}{2} - \frac{C(A + C)}{2(A - C)},\quad b = 1,$$
$$d = \frac{2\theta}{ln(A/C)},\quad c = d \cdot ln\left(\frac{A - C}{C\sqrt{AC}}\right). \tag{A4}$$

If $\frac{AB}{C^2} < 1$, the S_B (W_B) distribution should be employed, and the parameters are

$$a = \frac{x_1 + x_{-1}}{2} - \frac{b}{2} + \frac{C^2(A - B)}{2(C^2 - AB)},$$
$$b = \frac{C\sqrt{[(B + C)(A + C) - 4AB](B + C)(A + C)}}{C^2 - AB},$$
$$d = \frac{\theta}{cosh^{-1}\left[\frac{1}{2}\sqrt{(1 + C/A)(1 + C/B)}\right]},$$
$$c = d \cdot sinh^{-1}\left[\frac{C(A - B)\sqrt{(1 + C/A)(1 + C/B) - 4}}{2(C^2 - AB)}\right]. \tag{A5}$$

TABLE A1 The generalized Johnson system based on Weibull distribution.

		CDF
$\Psi(Z)$	–	$1-exp\left[-\left(\frac{Z+\mu}{\beta}\right)^{\alpha}\right]\quad(\mu=\beta\Gamma(1+1/\alpha))$
	W_U	$1-exp\left(-\left[\frac{\mu+c+d\cdot sinh^{-1}\left(\frac{X-a}{b}\right)}{\beta}\right]^{\alpha}\right)$
$F(X)$	W_L	$\frac{\alpha d}{\beta^{\alpha}}\cdot\frac{\left[\mu+c+d\cdot sinh^{-1}\left(\frac{X-a}{b}\right)\right]^{\alpha-1}}{\sqrt{(X-a)^2+b^2}}exp\left(-\frac{\left[\mu+c+d\cdot sinh^{-1}\left(\frac{X-a}{b}\right)\right]^{\alpha}}{\beta^{\alpha}}\right)$
	W_B	$a+b\cdot sinh\left(\frac{\beta\left[-ln(1-U)\right]^{1/\alpha}-\mu-c}{d}\right)$
		PDF
$\psi(Z)$	–	$\frac{\alpha}{\beta^{\alpha}}(Z+\mu)^{\alpha-1}exp\left[-\left(\frac{X+\mu}{\beta}\right)^{\alpha}\right]$
	W_U	$1-exp\left(-\left[\frac{\mu+c+d\cdot ln\left(\frac{X-a}{b}\right)}{\beta}\right]^{\alpha}\right)$
$f(X)$	W_L	$\frac{\alpha d}{\beta^{\alpha}}\cdot\frac{\left[\mu+c+d\cdot ln\left(\frac{X-a}{b}\right)\right]^{\alpha-1}}{X-a}exp\left(-\frac{\left[\mu+c+d\cdot ln\left(\frac{X-a}{b}\right)\right]^{\alpha}}{\beta^{\alpha}}\right)$
	W_B	$a+b\cdot exp\left(\frac{\beta\left[-ln(1-U)\right]^{1/\alpha}-\mu-c}{d}\right)$
		Quantile function
$\Psi^{-1}(U)$	–	$\beta\left[-ln(1-U)\right]^{1/\alpha}-\mu$
	W_U	$1-exp\left(-\left[\frac{\mu+c+d\cdot ln\left(\frac{X-a}{a+b-X}\right)}{\beta}\right]^{\alpha}\right)$
$F^{-1}(U)$	W_L	$\frac{\alpha bd}{\beta^{\alpha}}\cdot\frac{\left[\mu+c+d\cdot ln\left(\frac{X-a}{a+b-X}\right)\right]^{\alpha-1}}{(X-a)(a+b-X)}exp\left(-\frac{\left[\mu+c+d\cdot ln\left(\frac{X-a}{a+b-X}\right)\right]^{\alpha}}{\beta^{\alpha}}\right)$
	W_B	$a+b-\frac{b}{1+exp\left(\frac{\beta\left[-ln(1-U)\right]^{1/\alpha}-\mu-c}{d}\right)}$